DOI: 10.1002/ejic.201901070



Dissymmetric Cobalt Complexes

New Synthetic Route for Cobalt(III) Dissymmetric Bisalkynyl Complexes Based on Cobalt(III)(cyclam)(C₂NAP^{Mes})

Susannah D. Banziger, [a] Matthias Zeller, [a] and Tong Ren*[a]

Abstract: The synthesis and characterization of dissymmetric Co^{III}-bis-alkynyl complexes supported by cyclam (1,4,8,11-tetra-azacyclotetradecane) are reported. A series of *trans*-[Co(cyclam)-(C₂NAP^R)Cl]Cl were prepared from the reaction between [Co-(cyclam)Cl₂]Cl and HC₂NAP^R in the presence of Et₃N, where NAP^R is *N*-R-1,8-naphthalimide with R as mesityl (Mes, **1a**), methyl (Me, **1b**), 1-ethylpropyl (Pen, **1c**), 2-ethylhexyl (2-ethhex, **1d**), or *n*-octyl (Oct, **1e**). Treating compounds **1a** and **1b** with AgOTf in

NCCH₃ resulted in *trans*-[Co(cyclam)(C₂NAP^R)(NCCH₃)](OTf)₂ (**2a** and **2b**, respectively), while reactions with **1c**, **1d** and **1e** under the same conditions yielded only intractable mixtures. More soluble **2a** reacted further with HC₂Ar in the presence of Et₃N to afford *trans*-[Co(cyclam)(C₂NAP^R)(C₂Ar)](OTf) with Ar as C₆H₄-4-NMe₂ (**3a**), NAP^{Mes} (**3b**) and Ph (**3c**). All new complexes were characterized using X-ray diffraction (**1a**, **1c** and **3b**), IR, ¹H NMR, UV/Vis and fluorescent spectroscopy, and cyclic voltammetry.

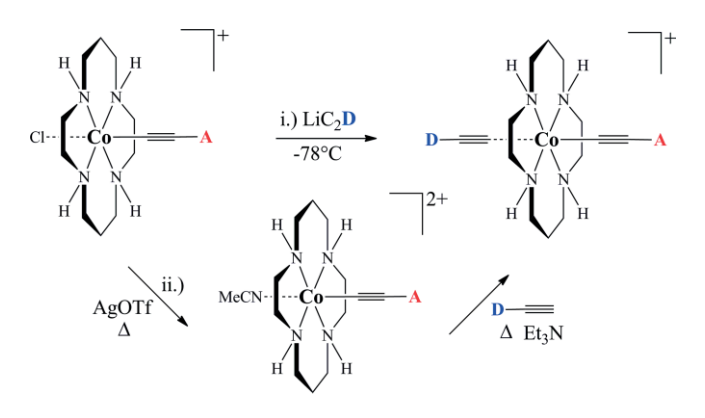
Introduction

The understanding of electron transfer processes is paramount to chemistry, biology and material sciences.[1,2] Photoinduced electron transfer (PET) has been very topical because of its relevance to both natural photosynthesis^[1] and photovoltaics.^[3] Recent years have seen efforts towards attenuation of intramolecular photo-induced electron transfer either through external stimuli such as pH change, [4] hydrogen bonding [5] or structural modification of the bridge between the donor and the acceptor.^[6] An interesting alternative approach is to modulate the evolution of electronic excited states through the excitation of a specific bond along the PET pathway. Working with a series of donor-bridge-acceptor (D-B-A) compounds with a trans-Pt^{II}bis-alkynyl bridge, Weinstein and co-workers demonstrated that the decay pathways of the PET excited state may be significantly attenuated by the IR excitation of the Pt-bound C≡C bonds.[7,8]

In addition to illustrating the control of PET processes using vibrational pumping, work of Weinstein also demonstrates the advantage of conjugated metal alkynyls as electronic and opto-electronic materials. [9,10] Importantly, the rigidity of metal alkynyls allows for unambiguous establishment of structure-property relationships. [11,12] Hence, bimetallic species bridged by oligo-yn-diyl have become a favorite target as prototypical molecular wires, [13] for which the precise distance dependence of metalmetal electronic couplings can be established using mixed valence theory. [14] Though rare, molecular conductance of metal

alkynyls has been measured in nanojunctions,^[15] and functional devices with metal alkynyls as the active species have been fabricated.^[16]

While the majority of the abovementioned examples are based on 4d and 5d metals, our laboratory has been exploring alkynyl chemistry based on M(cyclam) unit with M as 3d metals such as Cr, Fe, Co and Ni.^[17,18] Aiming at achieving PET attenuation in related 3d metal complexes, D-B-A compounds based on $Co^{[II]}(cyclam)$ have been selectively prepared in high yields^[17,18] through two different routes: i) stepwise alkynylation, with the first step proceeding under weak base conditions and the second utilizing lithiated acetylide^[19,20] and ii) stepwise alkynylation under weak base conditions via a triflate intermediate^[21,22] as shown in Scheme 1. Each synthetic route suffers from harsh conditions, with the most notable being (i) use of a strong base and (ii) high temperature. Previous work to synthesize the first dissymmetric D-B-A $Co^{[II]}(cyclam)$ complexes, where $D = C_6H_4$ -4- NR'_2 (R' = Me or Ph-4-OMe) and A = N-isopropyl-



Scheme 1. Syntheses of dissymmetric D-B-A compounds based on $Co^{III}(cyc-lam)$. Route i.) use of a strong base at low temp. Route ii.) use of a triflate intermediate in the presence of weak base and heat.

http://www.chem.purdue.edu/tren/

Supporting information and ORCID(s) from the author(s) for this article are available on the WWW under https://doi.org/10.1002/ejic.201901070.

[[]a] Dr. S. D. Banziger, Dr. M. Zeller, Prof. Dr. T. Ren Department of Chemistry, Purdue University, 560 Oval Drive, West Lafayette, IN 47906, USA E-mail: tren@purdue.edu





1,8-naphthalimide (NAP*i*Pr), could only be accomplished using the first route. [18] Since that time, our group has investigated the tuning of reactivity, crystallinity, and "robustness" of the naphthalimide unit through altering the alkyl group directly linked to the imide. Reported herein is the synthesis of new $Co^{III}(cyclam)(C_2NAP^R)$ species with R as mesityl (Mes, **1a**), methyl (Me, **1b**), 1-ethylpropyl (Pen, **1c**), 2-ethylhexyl (2-ethhex, **1d**), or *n*-octyl (Oct, **1e**) and a discussion on their properties and reactivity (Scheme 2). It should be noted that we have benefited from the early development of naphthalimide-acetylene chemistry by McAdam and co-workers, including Ni, Fe and Ru compounds of $C_2NAP^{Me[23]}$ and naphthalimide-acetylene ferrocenyl conjugates. [24,25]

Scheme 2. [Co(cyclam)(C₂NAP^R)Cl]Cl type compounds.

Results and Discussion

Synthesis

The general synthesis of 4-ethynyl-N-alkyl-1,8-naphthalimide (HC₂NAP^R) is illustrated in Scheme 3. It comprises the reaction between 4-bromonaphthalic anhydride and appropriate RNH₂ to yield 4-bromo-N-alkyl-1,8-naphthalimide, and the Sonogashira coupling between the latter and trimethylsilylacetylene. The preparations of 4-ethynyl-N-methyl-1,8-naphthalimide (HC_2NAP^{Me}) , [24] 4-ethynyl-N-2-ethylhexyl-1,8-naphthalimide (HC₂NAP^{2-ethhex}),^[26] and 4-ethynyl-*N*-octyl-1,8-naphthalimide (HC2NAPOct)[8] follow literature procedures. For 4-ethynyl-Nmesityl-1,8-naphthalimide (HC2NAPMes), the initial insertion of H₂NMes into the naphthalic anhydride requires 84 h of reflux in ethanol, five times longer than any other derivative reported herein. Desilylation of TMSC₂NAP^{Mes} formed HC₂NAP^{Mes} in high yield and dimerized NAP^{Mes}C₄NAP^{Mes} as a minor by-product. 4-ethynyltrimethylsilyl-N-1-ethylpropyl-1,8of naphthalimide (TMSC₂NAP^{Pen}) occurred within 20 min at room temperature; longer reaction times or extra heating resulted in degradation and formation of NAPPenC₄NAPPen. Synthetic details for both HC2NAPMes and HC2NAPPen are provided in the ESI.

Synthesis of mono acetylide Co^{III}(cyclam) compounds 1a-1e was accomplished under N₂ through the reaction of HC₂NAP^R (R is defined in Scheme 2) with [Co(cyclam)Cl₂]Cl in the presence of Et₃N.^[18] Except for **1b**, purification over silica resulted in bright orange microcrystalline solids in 45-63 % yield. Due to low solubility of 1b, its isolation was accomplished by addition of ether to the crude reaction mixture to yield a light orange powder in 48 % yield. Reaction of AgOTf (5 equiv.) with 1a and 1b in NCCH₃ resulted in [Co(cyclam)(C₂NAP^{Mes})- $(NCCH_3)](OTf)_2$ (2a) and $[Co(cyclam)(C_2NAP^{Me})(NCCH_3)](OTf)_2$ (2b), respectively, as yellow powders. Attempts to synthesize [Co(cyclam)(C₂NAP^R)(NCCH₃)](OTf)₂ type intermediates based on 1c-1e led to the consumption of the starting materials, but intractable products. Plausible causes of degradation include hydrolytic cleavage of the imido groups in NAPR and Co-C bond cleavage aided by Ag(I) coordination to the C=C bond. Hence, dissymmetric complexes based on NAP^{Pen}, NAP^{2-ethhex}, and NAP^{Oct} were not pursued further. The reaction between 2b and HC₂C₆H₄-4-NMe₂ in the presence of Et₃N afforded [Co-(cyclam)(C₂NAP^{Me})(C₂C₆H₄-4-NMe₂)]OTf as a light orange powder in 29 % yield. However, poor solubility of [Co(cyclam)-(C₂NAP^{Me})(C₂C₆H₄-4-NMe₂)]OTf made further characterization difficult. Hence, efforts to synthesize dissymmetric bis-alkynyls focused on the significantly more soluble NAP^{Mes} derivatives.

 $[Co(cyclam)(C_2NAP^{Mes})(C_2C_6H_4-4-NMe_2)]OTf$ (3a), [Co(cyclam)- $(C_2NAP^{Mes})_2]OTf$ (3b), and $[Co(cyclam)(C_2NAP^{Mes})(C_2Ph)]OTf$ (3c) were synthesized from 2a under N2 in the presence of excess HC₂Ar and Et₃N as shown in Scheme 4. Compounds **3b** and **3c** were isolated as bright yellow solids and 3a as a light orange solid. Low reaction yields for 3a (39 %) and 3b (11 %) were attributed to the hydroamination of -C≡C-NAP^{Mes} by Et₃N to form [Et₃NC₂H₂NAP^{Mes}]OTf, which was isolated and characterized (ESI). Hydroamination of alkynes in the presence of perchlorate salts to form vinyl tertiary amines was initially reported by Fischer in 1968. [27] This type of reactivity has been used in the literature to promote carboamination of alkynes in the presence of Pt,^[28] Pd. [29] and Au [30] catalysts. While reaction yields were lower than those for similar compounds synthesized using nBuLi, [20] this new reactivity unlocks the potential to target more exotic donor/ acceptor ligands that might not be stable in the presence of a strong nucleophile. Furthermore, symmetric bis-alkynyl by-products, formed by ligand scrambling, were not observed in the synthesis of 3a and 3c, regardless of the stoichiometry of the second alkynyl used. All new Co(cyclam) compounds (1a-1e and **3a-c**) are diamagnetic, consistent with a low spin Co^{III} center, which enables the characterization of these compounds using ¹H NMR. Additionally, these compounds were analyzed using ESI-MS and elemental analysis.

$$Br \longrightarrow 0 \quad i.) \longrightarrow 0 \quad ii.) \longrightarrow 0 \quad iii.) \longrightarrow 0 \quad iii.$$

Scheme 3. i.) 3 equiv. H_2NR , ethanol/2-propanol, reflux, 18–84 h; ii.) 2–3 equiv. HC_2SiMe_3 , iPr_2NH , 2 mol-% Cul, 2 mol-% Pd(PPh_3)₂Cl₂, 20 min-2 h; iii.) excess K_2CO_3 , MeOH, 30 min.





Scheme 4. i.) 1.1 equiv. HC₂NAP^{Mes}, Et₃N, CH₃OH:THF, reflux, 18 h; ii.) 5 equiv. AgOTf, NCCH₃, reflux, 16 h; iii.) 4 equiv. HC₂Ar, Et₃N, NCCH₃, reflux, 24 h.

Molecular Structures

Single crystals of **1a**, **1c** and **3b** were grown via slow diffusion of a less polar solvent into a polar concentrated solution of the respective compound; the molecular structures of cations are shown in Figure 1, Figure 2, and Figure 3, respectively. Selected bond lengths and angles are provided in Table 1, while the crystal data are listed in Table S1 (ESI). Single crystal structures of HC₂NAP^{Mes} and [Et₃NC₂H₂NAP^{Mes}]OTf were determined as well, and the details are provided in the ESI.

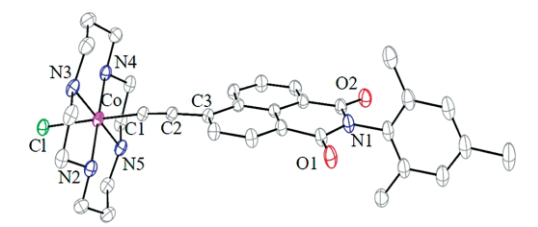


Figure 1. ORTEP plot of cation $[1a]^+$ at 30 % probability level; chloride counterions, hydrogen atoms, disorder, and solvent molecules are omitted for clarity.

Figure 2. ORTEP plot of cation [1c]* at 30 % probability level; chloride counterions, hydrogen atoms, disorder, and solvent molecules are omitted for clarity.

Figure 3. ORTEP plot of cation [**3b**]* at 30 % probability level (one of two crystallographically independent cations is shown); triflate counterions, hydrogen atoms, and solvent molecules are omitted for clarity.

Table 1. Selected bond lengths [Å] and angles [°] for compounds [1a]+, [1c]+ and [3b]+.

	[1a] ⁺	[1c] ⁺	[3b] ⁺
Co1-C1	1.859(3)	1.866 (5)	1.933(4)
Co1-N2	1.990(2)	1.974 (4)	1.982(4)
Co1-N3	1.973(2)	1.937 (4)	1.972(3)
Co1-N4	1.971(2)	1.981 (4)	-
Co1-N5	1.983(2)	2.019 (4)	_
Co1-Cl1	2.3154(5)	2.317 (3)	-
C1-C2	1.204(3)	1.213 (5)	1.210(5)
Cl1-Co-C1	176.76(8)	179.4 (3)	_
C1'-Co-C1	-	_	180.0
Co-C1-C2	174.0(2)	177.4 (7)	171.1(4)
C1-C2-C3	176.5(2)	178.6 (6)	170.4(4)

The Co centers of 1a, 1c and 3b assume pseudo-octahedral geometries with the alkynyl and Cl/alkynyl trans- to each other. Consistent with previous studies, the Co-C1 bond length is significantly longer in the bis-NAP^{Mes} species, **3b** [1.933(4) Å], compared to the mono-NAP^{Mes}, 1a [1.859(3) Å], which can be attributed to the trans-influence as the increased donor strength provided by the alkynyl compared to the CI in the axial position results in a weaker bond. [19,21,22,31-33] The influence of the electron withdrawing/donating character of the alkynyl ligand on the Co-C1 bond length can be observed across the literature with $[Co(cyclam)(C_2CF_3)_2]^+$ $(1.917)^{[34]} < [Co(cyclam)(C_2C_6F_5)_2]^+$ $(1.926)^{[22]}$ < **3b** (1.933) < $[Co(cyclam)(C_2C_6H_4-4-NMe_2)_2]^+$ $(1.942)^{[21]} < [Co(cyclam)(C_2Ph)_2]^+ (2.001)^{[35]}$ The electron withdrawing species (-CF₃, C₆F₅, and -NAP^{Mes}) have notably shortened bond lengths (Co-C) compared to the electron donating groups [-NMe2 and -N(Ph-4-OMe)2] due to reduced antibonding contribution from the $\pi(C \equiv C)$ to the Co $d\pi$. [19,31,36]

Crystallographic data consistently shows the mesityl group perpendicular to the naphthalimide ligand (Figure 1 and Figure 3), suggesting a sterically rigid structure. In contrast, flexible alkyl chains as seen in NAP^{Pen} or NAP*i*Pr can readily rotate, leaving the imido carbonyls more accessible to nucleophilic attack. Space filling models of [1a]⁺ and [1c]⁺ (Figure S3, ESI) illustrate how the methyl groups on the mesityl lock the ring into place.





Voltammetry

The CVs of compounds 1a, 3a, 3b, and HC2NAPMes are shown in Figure 4, and all exhibit a reversible reduction (A) based on the NAP^{Mes} ligand. The Co containing species (1a and 3a-3c) undergo three Co based events: one irreversible 1e⁻ oxidation $(Co^{+4/+3})$ and two irreversible $1e^-$ reductions $(Co^{+3/+2})$ and (Co^{+2/+1}) shown in the Figure S4 (ESI). The electrode potentials for these couples are listed in Table 2. Comparison of monoalkynyl (1a) to the bis-alkynyl species (3a-c), reveals that the first Co reduction shifts to significantly more negative potentials upon addition of a second alkynyl. This trend is consistent with previous observations and is attributed to the increased donor strength of an alkynyl vs. a chloro in the axial position. [20] Comparison of the HC₂NAP^{Mes} reduction potential (-1.52 V) to those of 1a and 3a-c validates the assignment of the reversible reduction at -1.66 V being localized on the naphthalimide moiety. Furthermore, it is clear from Figure 4 that 3b undergoes a reversible 2e- NAPMes-based reduction as the current at -1.66 V is approximately twice of those for 1a, 3a and HC₂NAP^{Mes}. The

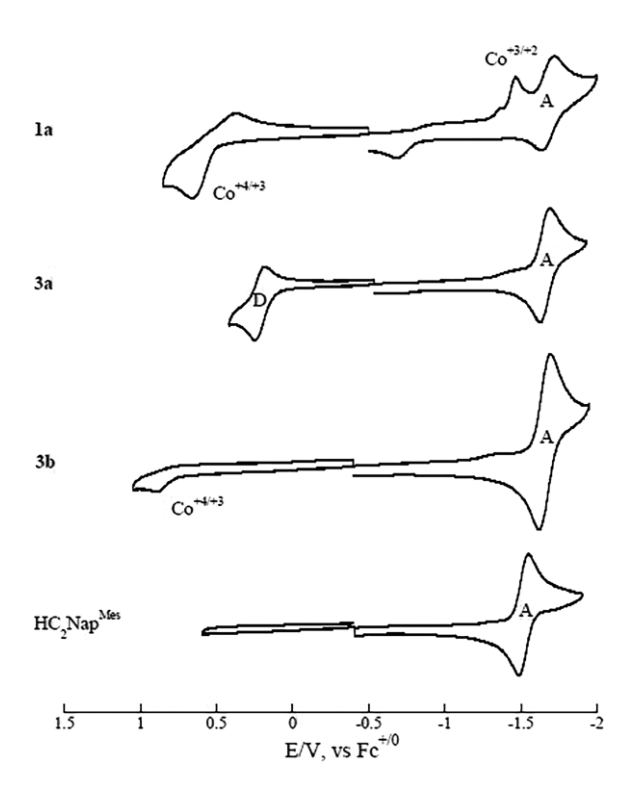


Figure 4. Cyclic voltammograms of 1a, 3a, 3b and HC_2NAP^{Mes} vs. Fc/Fc^+ in 1.0 mM NCCH_3 solutions with $0.1 \text{ M } [Bu_4N][PF_6]$ as the supporting electrolyte.

Table 2. Electrode potentials [V] for 1a, 3a, 3b, 3c, and HC₂NAP^{Mes}. [a]

Compound	$E_{1/2}(D)$	$E_{1/2}(A)$	$E_{pc}(Co^{+3/+2})$	$E_{pc}(Co^{+2/+1})$	$E_{pa}(Co^{+4/+3})$
1a	-	-1.69 (0.10)	-1.47	-2.19	0.66
3a	0.22 (0.07)	-1.66 (0.06)	-2.15	-2.26	0.73
3b	-	-1.66 (0.08)	-2.16	-2.32	0.89
3с	_	-1.66 (0.08)	-1.85	-2.30	1.17
HC ₂ NAP ^{Mes}	-	-1.52 (0.06)	-	-	-

[[]a] Reported vs. $Fc^{+/0}$ in NCCH₃ with 0.1 M [Bu₄N][PF₆] as the supporting electrolyte. Peak separations ($E_{pa} - Ep_c$) for reversible couples are shown in brackets.

quasi-reversible oxidation couple at 0.22 V for the complex ${\bf 3a}$ is assigned to the donor ($-C_6H_4$ -4-NMe $_2$) based on related literature examples of [Co(cyclam)($C_2C_6H_4$ -4-NMe $_2$) $_2$]⁺ and [Co-(cyclam)($C_2C_6H_4$ -4-NMe $_2$)($C_2C_6F_5$)]^{+,[22]} Consistent with observations for [Co(cyclam)($C_2NAPiPr$)($C_2C_6H_4$ -4-NMe $_2$)]CI,^[20] this assignment suggests that the HOMO and LUMO for compound ${\bf 3a}$ reside on the donor and acceptor, respectively, and the electrochemical HOMO-LUMO gap [$E_g=E_{1/2}(D)-E_{1/2}(A)$] can be estimated as 1.88 V.

UV/Vis and Emission Spectra

Absorption and emission spectra were collected at room temperature in CH_2CI_2 under ambient conditions and λ_{max} for these spectra were recorded for **1a**, **3a–c**, $TMSC_2NAP^{Mes}$, HC_2NAP^{Mes} , $[Et_3NC_2H_2NAP^{Mes}]$ OTf and $NAP^{Mes}C_4NAP^{Mes}$ in Table 3. UV/Vis spectra of all Co-based compounds are shown in Figure 5 (**1a** and **3a–c**), while those of $TMSC_2NAP^{Mes}$, $[Et_3NC_2H_2NAP^{Mes}]$ OTf and $NAP^{Mes}C_4NAP^{Mes}$ are given in Figure S5 (ESI). The absorption spectrum of $TMSC_2NAP^{Mes}$ features an intense peak at 360 nm, which is attributed to the π – π * transition localized on $NAP^{Mes}[^{[8,20]}]$ All Co-based compounds, **1a** and **3a–c**, display broad absorption bands around 400 nm. TD-DFT calculations performed on related compounds, $[Co(cyclam)(C_2NAPiPr)CI]CI$, $[Co(cyclam)(C_2NAPiPr)(C_2C_6H_4-4-NMe_2)]CI$ and $[Co(cyclam)(C_2NAPiPr)(C_2C_6H_4-4-N(Ph-4-OMe)_2)]CI$, indicate that this transition is predominantly a NAP^{Mes} based π – π * transition. $[^{[20]}]$

Table 3. Absorption and emission maxima (λ /nm) in CH₂Cl₂.

Compound	λ_{abs}	$\lambda_{em/}\lambda_{ex}$
1a	396	441/390
3a	399	441/390
3b	401	433/390
3c	397	441/390
TMSC ₂ NAP ^{Mes}	358/376	399/360
HC ₂ NAP ^{Mes}	351/368	405/340
NAP ^{Mes} C ₄ NAP ^{Mes}	395/425	439/390
[Et ₃ NC ₂ H ₂ NAP ^{Mes}]OTf	350	410/330

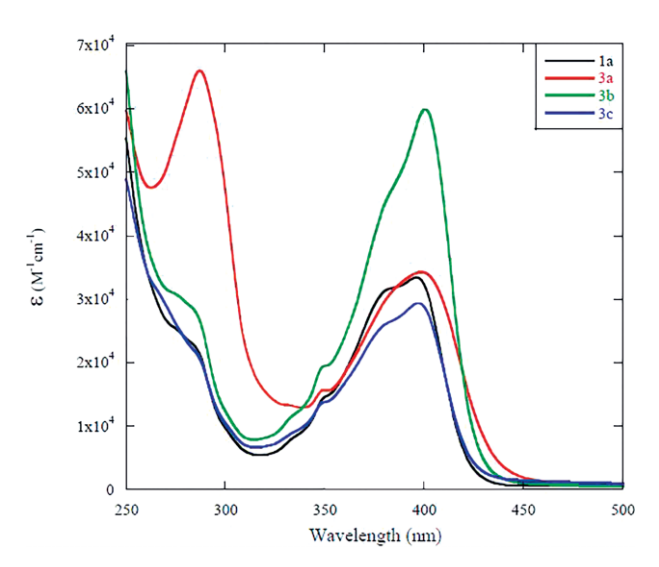


Figure 5. Absorption spectra of ${\bf 1a}$ (black), ${\bf 3a}$ (red), ${\bf 3b}$ (green), and ${\bf 3c}$ (blue) in ${\rm CH_2Cl_2}$.





assignment is also consistent with $Pt^{II}(PnBu_3)_2(C_2NAP^{Oct})$ type complexes reported by Weinstein and co-workers, where the lowest energy transition was observed at 430 nm and was attributed to mixed metal-ligand-to-ligand charge transfer (ML/L'CT). Generally, $Co^{III}(cyclam)$ acetylides display a d-d transition around 450–500 nm, with higher energy transitions occurring for the bis-acetylide complexes and the lower energy for the mono-acetylides. $P_2(19,21,22,31,32,36,37)$ However, only compound $P_3(19,21,22,31,32,36,37)$ However, only com

Use of a simple chromophore as the acceptor allows for analysis of steady-state emission, which may reveal the effect the Co^{III}(cyclam) bridge and the donor (-C₆H₄-4-NMe₂) have on the acceptor (NAPMes) emission. As illustrated by the normalized emission spectra of 1a, 3a and TMSC₂NAP^{Mes} in Figure 6, the emission profiles of 1a and 3a-c resemble those of the X- C_2NAP^{Mes} species (X = TMS or H), but were significantly redshifted (ca. 50 nm). The relatively small Stokes shift between λ_{abs} and λ_{em} suggests that the observed emission originates from the excited state around 400 nm. Furthermore, the similarity between the emission of 1a and 3a suggests that the C₆H₄-4-NMe₂ donor does not significantly affect the electronic states of Co bound -C2NAPMes. Similar findings were reported for the analogous compounds bearing NAPiPr, with fluorescent guantum yields ($\Phi_{\rm fl}$) in CH₂Cl₂ on the order of 0.43–0.66 % for the Co^{III}(cyclam)(C₂NAPiPr) compounds and 42 % for HC₂NAPiPr.^[20] The dimerized forms of NAPR ligand, namely NAPR-C4-NAPR (R = *n*Bu or Ph), were reported to have $\Phi_{\rm fl}$ on the order of 83 % and 101 %, respectively.[38] While quantum yields were not recorded for this series, compounds 1a and 3a-c were observed to have extremely weak emission compared to the organic species listed in Table 3. Quenching of fluorophore emission due to the presence of a metal has also been observed by the Weinstein group, who recorded a Φ_{fl} of 5.5 % for a $Pt^{II}(PnBu_3)_2(C_2NAP^{Oct})$ D-B-A species, [8,9] and by McAdam and co-workers who recorded a $\Phi_{\rm fl}$ of 0.11 % and 0.24 % for naphthalimide species linked to ferrocene.[24]

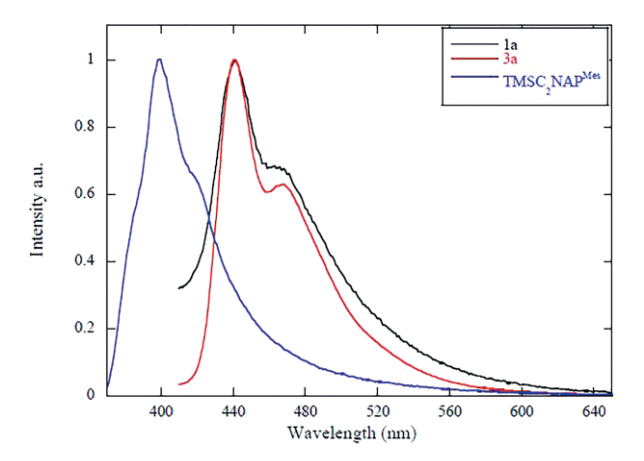


Figure 6. Normalized emission spectra of ${\bf 1a}$ vs. ${\bf 3a}$ and ${\sf TMSC_2NAP^{Mes}}$ in ${\sf CH_2CI_2}.$

Conclusion

Described in this contribution are several new [Co^{III}(cyclam)- $(C_2NAP^R)CI_1^+$ type complexes (R = Mes, Me, Pen, 2-ethhex, Oct) that exhibit improved crystallinity and reactivity over [Co^{III}(cyclam)(C₂NAP*i*Pr)Cl]⁺.[20] Careful tuning of the alkyl group on the naphthalimide moiety revealed that -C2NAPMes based complexes performed the best in the aforementioned categories. The increased stability afforded by the mesityl group allows for selective synthesis of the [Co^{III}(cyclam)(C₂NAP^{Mes})(C₂Ar)]⁺ type complexes under weak base conditions through a triflate intermediate. Furthermore, the perpendicular orientation of the mesityl ring in respect to the naphthalimide group prevents π - π stacking thereby increasing solubility and crystallinity. These encouraging results suggest that possible synthetic strategies for the next generation of D-B-A complexes include i) Hagihara coupling (Cul/organic amine) as a variation of the dehydrohalogenation reactions (used to couple arylalkynyls to cobalamin^[39]) and ii) organo-tin activated arylalkynyls (used by Lewis and co-workers^[12,40] to synthesize *trans*-Ru^{II} acetylides).

Experimental Section

Materials: Literature procedures were followed in the preparations of [Co(cyclam)Cl₂]Cl,^[41] 4-ethynyl-*N*-methyl-1,8-naphthalimide,^[24] 4-ethynyl-*N*-2-ethylhexyl-1,8-naphthalimide,^[26] and 4-ethynyl-*N*-octyl-1,8-naphthalimide.^[8] Diisopropylamine and triethylamine were purchased from ACROS Organics and Fisher Chemical, respectively, and distilled from potassium hydroxide before use. 4-Ethynyl-*N*,*N*-dimethylaniline was purchased from Sigma Aldrich. Phenylacetylene was purchased from GFS Chemicals. All alkynylation reactions were carried out using Schlenk techniques under dry N₂.

Physical Measurements: UV/Vis-NIR spectra were obtained with a JASCO V-670 UV/Vis-NIR spectrophotometer. Infrared spectra were obtained on a JASCO FT-IR 6300 spectrometer via ATR on a ZnSe crystal. ESI-MS was carried out on an Advion Mass Spectrometer. 1 H NMR spectra were recorded on a Varian INOVA300 NMR with chemical shifts (δ) referenced to the solvent signal (CD₃OD at 4.88 and 3.31 ppm; CDCl₃ at 7.26 ppm). Cyclic voltammograms were recorded in 0.1 $^{\rm M}$ $^{\rm M}$ Bu₄NPF₆ and 1.0 mM cobalt species solution (CH₃CN, Ar degassed) using a CHI620A voltammetric analyzer with a glassy carbon working electrode (diameter = 2 mm), Pt-wire counter electrode, and an Ag/AgCl reference electrode with ferrocene used as an external reference. Emission studies were measured on a Varian Cary Eclipse fluorescence spectrophotometer.

Synthesis of [Co(cyclam)(C₂NAP^{Mes})CI]CI (1a): [Co(cyclam)CI₂]CI (645 mg, 1.77 mmol) was dissolved in 50 mL CH₃OH to which a 10 mL solution of THF containing 4-ethynyl-*N*-mesityl-1,8-naphthalimide (677 mg, 2.0 mmol) was added and purged with N₂. Upon addition of Et₃N (4.0 mL, 30 mmol) the solution darkened and was refluxed for 18 h. Silica plug purification with CH₃OH/CH₂CI₂ (v/v, 1:9) eluted the product as an orange band. Recrystalization from CH₃OH/CH₂CI₂ (v/v, 1:1) and ether yielded 600 mg of **1** as an orange solid (51 % based on [Co(cyclam)CI₂]CI). ESI-MS: [M]⁺, 630.2; ¹H NMR (300 MHz, [D]methanol) δ = 9.08 (d, J = 9.0 Hz, 1H), 8.65 (d, J = 7.4 Hz, 1H), 8.54 (d, J = 7.9 Hz, 1H), 8.04 (d, J = 7.9 Hz, 1H), 8.00–7.90 (m, 1H), 7.06 (s, 2H), 5.38 (s, 4H), 3.10–2.90 (m, 4H), 2.89–2.64 (m, 14H), 2.57 (d, J = 13.3 Hz, 2H), 2.37 (s, 3H), 2.04 (s, 6H). Visible spectrum, λ_{max} (nm, ε (м⁻¹ cm⁻¹)): 396 (33,400), 480 (534); IR (cm⁻¹): \tilde{v} = O: 1652 (s), 1700 (s); C≡C: 2103 (s). Elem. Anal. found (calcd.) for





 $C_{34}H_{44}N_5O_3CoCl_4$ (**1a·** H_2O ·C H_2Cl_2): C, 53.34 (52.93); H, 5.79 (5.75); N, 9.47 (9.08).

Synthesis of [Co(cyclam)(C2NAPPen)Cl]Cl (1c): [Co(cyclam)Cl2]Cl (99.5 mg, 0.27 mmol) was dissolved in 50 mL CH₃OH containing 0.7 mL (5.0 mmol) Et₃N. The solution was purged with N₂, then 4-ethynyltrimethylsilyl-N-1-ethylpropyl-1,8-naphthalimide (115 mg, 0.32 mmol) was added and the solution was refluxed for 16 h. Silica plug purification with CH₃OH/CH₂Cl₂ (v/v, 1:5) eluted the product as an orange band. Recrystallization from CH₃OH/CH₂Cl₂ (v/v, 1:1) and ether yielded 79 mg of 1c as an orange crystalline solid (47 % based on [Co(cyclam)Cl₂]Cl). ESI-MS: [M]⁺, 584.2; ¹H NMR (300 MHz, [D]methanol) $\delta = 8.97$ (d, J = 7.2 Hz, 1H), 8.58 (d, J = 6.8 Hz, 1H), 8.47 (d, J = 7.6 Hz, 1H), 7.97 (d, J = 7.7 Hz, 1H), 7.94–7.82 (m, 1H), 5.33 (s br, 4H), 5.06–5.01 (m, 1H), 2.88–2.69 (m, 14H), 2.26 (dd, J =13.8, 7.5 Hz, 2H), 2.12–1.95 (m, 4H), 1.89 (dd, J = 13.5, 5.9 Hz, 2H), 1.77–1.65 (m, 2H), 0.87 (t, J = 7.4 Hz, 6H). Visible spectrum, $\lambda_{\rm max}$ (nm, ε (M^{-1} cm⁻¹)): 391 (27,900), 483 (245); IR (cm⁻¹): \tilde{v} = O: 1647 (s), 1684 (s); C≡C: 2109 (s). Elem. Anal. found (calcd.) for C_{29.5}H₄₁N₅O₂CoCl₃ (**1c·**0.5CH₂Cl₂): C, 53.51 (53.45); H, 6.61 (6.23); N, 10.72 (10.56).

Synthesis of [Co(cyclam)(C2NAP2-ethhex)CI]CI (1d): [Co(cyclam)Cl₂]Cl (150 mg, 0.41 mmol) was dissolved in 80 mL CH₃OH to which a 10 mL solution of THF containing 4-ethynyl-N-2-ethylhexyl-1,8-naphthalimide (138 mg, 0.41 mmol) was added and purged with N₂. Upon addition of Et₃N (1.0 mL, 7.5 mmol) the solution darkened and was refluxed for 18 h. Silica plug purification with CH3OH/ CH₂Cl₂ (v/v, 1:6) eluted the product as an orange band. Recrystallization from CH₃OH/CH₂Cl₂ (v/v, 1:1) and ether yielded 122 mg of 1d as an orange solid (45 % based on [Co(cyclam)Cl₂]Cl). ESI-MS: [M]⁺, 626.3; ¹H NMR (300 MHz, [D]methanol) δ = 8.98 (d, J = 8.3 Hz, 1H), 8.58 (d, J = 6.9 Hz, 1H), 8.47 (d, J = 7.4 Hz, 1H), 7.97 (d, J =7.8 Hz, 1H), 7.90–7.83 (m, 1H), 5.34 (s, 4H), 4.10 (d, J = 7.2 Hz, 2H), 2.93-2.71 (m, 16H), 2.01 (d, J = 16.7 Hz, 4H), 1.73-1.68 (m, 1H), 1.37(dd, J = 14.8, 7.2 Hz, 8H), 1.04–0.83 (m, 6H). Visible spectrum, λ_{max} (nm, ε (M⁻¹ cm⁻¹)): 392 (24,500), 480 (253); IR (cm⁻¹): \tilde{v} = O: 1646 (s), 1691 (s); C≡C: 2101 (s). Elem. Anal. found (calcd.) for $C_{35}H_{56}N_5O_4CoCl_8$ (1d-2H₂O-3CH₂Cl₂): C, 43.96 (44.09); H, 5.75 (5.92); N, 7.99 (7.35).

Synthesis of [Co(cyclam)(C2NAPOct)Cl]Cl (1e): [Co(cyclam)Cl2]Cl (500 mg, 1.4 mmol) was dissolved in 90 mL CH₃OH and 4 mL Et₃N (30 mmol) to which 4-ethynyl-N-octyl-1,8-naphthalimide (513 mg, 1.5 mmol) was added and purged with N2. The solution was refluxed for 18 h. Silica plug purification with CH₃OH/CH₂Cl₂ (v/v, 1:5) eluted the product as an orange band. Recrystallization from CH₃OH/CH₂Cl₂ (v/v, 1:1) and ether yielded 345 mg of 1e as an orange solid (63 % based on [Co(cyclam)Cl₂]Cl). ESI-MS: [M]⁺, 626.3; ¹H NMR (300 MHz, [D]methanol) δ = 8.92 (d, J = 8.2 Hz, 1H), 8.53 (d, J = 7.1 Hz, 1H), 8.42 (d, J = 7.8 Hz, 1H), 7.93 (d, J = 7.7 Hz, 1H),7.89-7.79 (m, 1H), 5.34 (s, 4H), 4.17-4.06 (m, 2H), 2.99-2.67 (m, 18H), 2.10-1.98 (m, 2H), 1.74-1.70 (m, 2H), 1.42-1.29 (m, 10H), 0.90 (d, J =7.4 Hz, 3H). Visible spectrum, λ_{max} (nm, ε (M^{-1} cm⁻¹)): 393 (23,900), 482 (228); IR (cm⁻¹): $\tilde{v} = 0$: 1647 (s), 1684 (s); C=C: 2110 (s). Elem. Anal. found (calcd.) for $C_{34}H_{50}N_5O_2CoCl_6$ (1e-2CH₂Cl₂): C, 48.77 (49.06); H, 6.13 (6.05); N, 8.92 (8.41).

Synthesis of [Co(cyclam)(C₂NAP^{Mes})(NCCH₃)]OTf₂ (2a): [Co-(cyclam)(C₂NAP^{Mes})Cl]Cl, compound **1a** (323 mg, 0.49 mmol) was dissolved in 60 mL of CH₃CN and purged with N₂. Upon addition of AgOTf (620 mg, 2.41 mmol) the solution was refluxed for 16 h. The solution was filtered through celite with CH₃CN and concentrated. Recrystallization from CH₃CN and ether yielded 287 mg of **2a** as a yellow solid (63 % based on **1a**). ESI-MS: [M – OTf]⁺, 744.2.

Synthesis of [Co(cyclam)(C2NAPMes)(C2-4-C6H4NMe2)]Cl (3a): In a 50 mL round-bottomed flask, 2a (95 mg, 0.11 mmol) was dissolved in 20 mL CH₃CN and purged with N₂. After addition of Et₃N (0.9 mL, 6.6 mmol) and HC₂-C₆H₄-NMe₂ (62 mg, 0.43 mmol) the solution was refluxed for 24 h. Purification over a silica plug (SiO₂, CH₃OH/EtOAc v/v, 1:5) eluted the desired product as a light orange band. Recrystallization from CH₃CN/CH₂Cl₂ (v/v, 1:1) and ether yielded 43 mg of 3a as a light orange solid (39 % based on 2a). ESI-MS: [M]+, 741.3; ¹H NMR (300 MHz, [D]methanol) δ = 9.22 (d, J = 8.4 Hz, 1H), 8.66 (d, J = 6.9 Hz, 1H), 8.55 (d, J = 8.3 Hz, 1H), 8.06 (d, J = 7.7 Hz, 1H),7.98-7.91 (m, 1H), 7.38 (d, J = 8.8 Hz, 2H), 7.06 (s, 2H), 6.72 (d, J = 8.5 Hz, 2H), 4.86 (s, 4H), 2.94 (s, 6H), 2.76-2.68 (m, 12H), 2.65–2.52 (m, 8H), 2.37 (s, 3H), 2.06 (s, 6H). Visible spectrum, λ_{max} (nm, ε (m $^{-1}$ cm $^{-1}$)): 287 (66,000), 399 (34,300); IR (cm $^{-1}$): $\tilde{\nu}$ = O: 1654 (s), 1699 (s); C≡C: 2087 (w). Elem. Anal. found (calcd.) for C₄₅H₅₂N₆O₅CoCl₂SF₃ (**3a·**CH₂Cl₂): C, 55.06 (55.39); H, 5.60 (5.37); N, 8.61 (8.99).

Synthesis of [Co(cyclam)(C₂NAP^{Mes})₂]Cl (3b): In a 100 mL round-bottomed flask, **2a** (150 mg, 0.16 mmol) was dissolved in 60 mL CH₃CN and purged with N₂. After addition of Et₃N (1.5 mL, 7.9 mmol) and HC₂NAP^{Mes} (120 mg, 0.35 mmol) the solution was refluxed for 16 h. Purification over a silica plug (SiO₂, CH₃OH/CH₂Cl₂ v/v, 1:7) eluted the desired product as a yellow band. Recrystallization from CH₃CN/CH₂Cl₂ (v/v, 1:1) and ether yielded 20 mg of **3b** as a yellow solid (11 % based on **2a**). ESI-MS: [M]⁺, 935.4; ¹H NMR (300 MHz, [D]methanol) δ = 9.24 (d, J = 8.8 Hz, 2H), 8.68 (d, J = 7.5 Hz, 2H), 8.58 (d, J = 7.9 Hz, 2H), 8.11 (d, J = 8.3 Hz, 2H), 8.01–7.93 (m, 2H), 7.07 (s, 4H), 5.61 (s, 4H), 3.13–3.06 (m, 3H), 2.85–2.66 (m, 17H), 2.37 (s, 6H), 2.07 (s, 12H). Visible spectrum, λ _{max} (nm, ε (ω ⁻¹ cm⁻¹)): 401 (59,900); IR (cm⁻¹): \tilde{v} = O: 1655 (m), 1698 (m); C≡C: 2086 (w). Elem. Anal. found (calcd.) for C₆₁H₆₃N₇O₇CoCl₄SF₃ (**3b**•2CH₂Cl₂·CH₃CN): C, 56.06 (56.53); H, 5.06 (4.90); N, 7.41 (7.57).

Synthesis of [Co(cyclam)(C2NAPMes)(C2Ph)]CI (3c): In a 100 mL round-bottomed flask, 2a (150 mg, 0.16 mmol) was dissolved in 30 mL CH₃CN and purged with N₂. After addition of Et₃N (1.5 mL, 7.9 mmol) and HC₂Ph (0.1 mL, 11 mmol) the solution was refluxed for 16 h. Purification over a silica plug (SiO₂, CH₃OH/CH₂Cl₂ v/v, 1:8) eluted the desired product as a yellow band. Recrystallization from CH₃CN/CH₂Cl₂ (v/v, 1:1) and ether yielded 81 mg of 3c as a yellow solid (60 % based on 2a). ESI-MS: [M]+, 698.3; ¹H NMR (300 MHz, [D]methanol) $\delta = 9.09$ (d, J = 7.1 Hz, 1H), 8.66 (d, J = 6.3 Hz, 1H), 8.54 (d, J = 8.1 Hz, 1H), 8.06 (d, J = 6.9 Hz, 1H), 8.03-7.92 (m, 2H), 7.52 (d, J = 8.8 Hz, 1H), 7.35–7.16 (m, 3H), 7.06 (s, 2H), 5.31 (s br, 4H), 3.02-2.69 (m, 18H), 2.60-2.54 (m, 2H), 2.37 (s, 3H), 2.06 (s, 6H). Visible spectrum, $\lambda_{\rm max}$ (nm, ε (M $^{-1}$ cm $^{-1}$)): 397 (29,400); IR (cm $^{-1}$): \tilde{v} = O: 1655 (s), 1699 (s); C=C: 2096 (s). Elem. Anal. found (calcd.) for $C_{47}H_{55}N_6O_5CoCl_6SF_3$ (3c-3CH₂Cl₂-CH₃CN): C, 49.09 (49.32); H, 4.23 (4.84); N, 6.98 (7.34).

X-ray Crystallographic Analysis: Single crystals of **1a** were obtained from the slow diffusion of diethyl ether into a CH_2CI_2/CH_3OH (v/v, 1:1) solution. Single crystals of **1c** were grown from slow diffusion of diethyl ether/hexanes (v/v 2:1) into a CH_3OH solution. Single crystals of **3b** were grown from slow diffusion of hexanes into a CH_2CI_2/CH_3OH (v/v, 2:1) solution. Single crystals of HC_2NAP^{Mes} were grown from slow evaporation of a $CH_2CI_2/hexanes$ (v/v 1:2) solution. Single crystals of $[Et_3NC_2H_2NAP^{Mes}]OTf$ were grown from slow diffusion of diethyl ether into a $CH_3CN/MeOH$ (v/v 1:1) solution. X-ray diffraction data for **1a**, **1c** and $[Et_3NC_2H_2NAP^{Mes}]OTf$ was obtained on a Bruker Quest diffractometer with $Mo-K_{\alpha}$ radiation ($\lambda = 0.71073 \text{ Å}$) at 150K. X-ray diffraction data for **3b** and HC_2NAP^{Mes} were obtained on a Bruker Quest diffractometer with $Cu-K_{\alpha}$ radiation ($\lambda = 1.54178 \text{ Å}$) at 150K. Data were collected; reflections were





indexed and processed using APEX3.^[42] The space groups were assigned and the structures were solved by direct methods using XPREP within the SHELXTL suite of programs^[43] and refined using Shelxl and Shelxle.^[44] Additional crystallographic data for HC₂NAP^{Mes}, [Et₃NC₂H₂NAP^{Mes}]OTf, **1a**, **1c** and **3b** are provided in Table S1 and Table S2 and in the SI (handling of H atoms, description of disorder, twinning and special refinement details).

CCDC 1937327 (for ${\bf 1a}$), 1937328 (for ${\bf 1c}$), 1937329 (for ${\bf 3b}$), 193730 (for HC_2NAP^{Mes}), and 193731 (for $[Et_3NC_2H_2NAP^{Mes}]OTf$) contain the supplementary crystallographic data for this paper. These data can be obtained free of charge from The Cambridge Crystallographic Data Centre.

Acknowledgments

We gratefully acknowledge financial support from the National Science Foundation (CHE 1764347 for research and CHE 1625543 for X-ray diffractometers). We would like to thank Lindsey A. Miller and Brandon L. Mash for assistance with X-ray data collection. S. D. B. thanks Purdue University for a *Cagiantas Fellowship*.

Keywords: Cobalt · Dissymmetric complexes · Alkyne ligands · Electrochemistry · Synthesis design

- [1] M. R. Wasielewski, Chem. Rev. 1992, 92, 435-461.
- [2] P. F. Barbara, T. J. Meyer, M. A. Ratner, J. Phys. Chem. 1996, 100, 13148–13168; B. Albinsson, J. Mårtensson, J. Photochem. Photobiol. C 2008, 9, 138–155.
- [3] A. Hagfeldt, M. Gratzel, Acc. Chem. Res. 2000, 33, 269–277.
- [4] Y. Gabe, Y. Urano, K. Kikuchi, H. Kojima, T. Nagano, J. Am. Chem. Soc. 2004, 126, 3357–3367.
- [5] J. L. Sessler, B. Wang, A. Harriman, J. Am. Chem. Soc. 1995, 117, 704-714.
- [6] A. C. Benniston, A. Harriman, Chem. Soc. Rev. 2006, 35, 169–179.
- [7] M. Delor, P. A. Scattergood, I. V. Sazanovich, A. W. Parker, G. M. Greetham, A. J. H. M. Meijer, M. Towrie, J. A. Weinstein, *Science* 2014, 346, 1492– 1495.
- [8] P. A. Scattergood, M. Delor, I. V. Sazanovich, O. V. Bouganov, S. A. Tikhomirov, A. S. Stasheuski, A. W. Parker, G. M. Greetham, M. Towrie, E. S. Davies, A. J. H. M. Meijer, J. A. Weinstein, *Dalton Trans.* 2014, 43, 17677–17693.
- [9] A. Haque, R. A. Al-Balushi, I. J. Al-Busaidi, M. S. Khan, P. R. Raithby, Chem. Rev. 2018, 118, 8474–8597.
- [10] C.-L. Ho, Z.-Q. Yu, W.-Y. Wong, Chem. Soc. Rev. 2016, 45, 5264–5295; P. J. Low, M. I. Bruce, Adv. Organomet. Chem. 2001, 48, 71–288; B. Pigulski, N. Gulia, S. Szafert, Eur. J. Org. Chem. 2019, 1420–1445; A. Triadon, G. Grelaud, N. Richy, O. Mongin, G. J. Moxey, I. M. Dixon, X. Yang, G. Wang, A. Barlow, J. Rault-Berthelot, M. P. Cifuentes, M. G. Humphrey, F. Paul, Organometallics 2018, 37, 2245–2262; A. Haque, R. A. Al-Balushi, M. S. Khan, J. Organomet. Chem. 2019, 897, 95–106.
- [11] S. Szafert, J. A. Gladysz, Chem. Rev. 2003, 103, 4175–4206; S. Szafert, J. A. Gladysz, Chem. Rev. 2006, 106, PR1–PR33.
- [12] N. J. Long, C. K. Williams, Angew. Chem. Int. Ed. 2003, 42, 2586–2617; Angew. Chem. 2003, 115, 2690.
- [13] J.-P. Launay, Chem. Soc. Rev. 2001, 30, 386–397; T. Ren, Organometallics 2005, 24, 4854–4870; K. Costuas, S. Rigaut, Dalton Trans. 2011, 40, 5643– 5658; Y. Tanaka, M. Akita, Coord. Chem. Rev. 2019, 388, 334–342.
- [14] R. Dembinski, T. Bartik, B. Bartik, M. Jaeger, J. A. Gladysz, J. Am. Chem. Soc. 2000, 122, 810–822; M. I. Bruce, P. J. Low, K. Costuas, J.-F. Halet, S. P. Best, G. A. Heath, J. Am. Chem. Soc. 2000, 122, 1949–1962; Z. Cao, B. Xi, D. S. Jodoin, L. Zhang, S. P. Cummings, Y. Gao, S. F. Tyler, P. E. Fanwick, R. J. Crutchley, T. Ren, J. Am. Chem. Soc. 2014, 136, 12174–12183.

- [15] T. L. Schull, J. G. Kushmerick, C. H. Patterson, C. George, M. H. Moore, S. K. Pollack, R. Shashidhar, J. Am. Chem. Soc. 2003, 125, 3202–3203; A. S. Blum, T. Ren, D. A. Parish, S. A. Trammell, M. H. Moore, J. G. Kushmerick, G.-L. Xu, J. R. Deschamps, S. K. Pollack, R. Shashidhar, J. Am. Chem. Soc. 2005, 127, 10010–10011; A. K. Mahapatro, J. Ying, T. Ren, D. B. Janes, Nano Lett. 2008, 8, 2131–2136; Y. Tanaka, Y. Kato, T. Tada, S. Fujii, M. Kiguchi, M. Akita, J. Am. Chem. Soc. 2018, 140, 10080–10084; B. Kim, J. M. Beebe, C. Olivier, S. Rigaut, D. Touchard, J. G. Kushmerick, X.-Y. Zhu, C. D. Frisbie, J. Phys. Chem. C 2007, 111, 7521–7526.
- [16] F. B. Meng, Y. M. Hervault, Q. Shao, B. H. Hu, L. Norel, S. Rigaut, X. D. Chen, Nat. Commun. 2014, 5, Art. 3023; H. Zhu, S. J. Pookpanratana, J. E. Bonevich, S. N. Natoli, C. A. Hacker, T. Ren, J. S. Suehle, C. A. Richter, Q. Li, ACS Appl. Mater. Interfaces 2015, 7, 27306–27313.
- [17] T. Ren, Chem. Commun. 2016, 52, 3271-3279.
- [18] S. D. Banziger, T. Ren, J. Organomet. Chem. 2019, 885, 39-48.
- [19] S. D. Banziger, T. D. Cook, S. N. Natoli, P. E. Fanwick, T. Ren, J. Organomet. Chem. 2015, 799–800, 1–6.
- [20] S. D. Banziger, X. Li, J. Valdiviezo, M. Zeller, P. Zhang, D. N. Beratan, I. Rubtsov, T. Ren, *Inorg. Chem.* 2019, 58, 15487–15497.
- [21] S. N. Natoli, M. Zeller, T. Ren, Inorg. Chem. 2016, 55, 5756-5758.
- [22] S. N. Natoli, M. Zeller, T. Ren, Inorg. Chem. 2017, 56, 10021-10031.
- [23] C. J. McAdam, A. R. Manning, B. H. Robinson, J. Simpson, *Inorg. Chim. Acta* 2005, 358, 1673–1682.
- [24] C. J. McAdam, J. L. Morgan, B. H. Robinson, J. Simpson, P. H. Rieger, A. L. Rieger, Organometallics 2003, 22, 5126–5136.
- [25] C. J. McAdam, B. H. Robinson, J. Simpson, T. Tagg, Organometallics 2010, 29, 2474–2483.
- [26] A. Saini, K. R. J. Thomas, RSC Adv. 2016, 6, 71638-71651.
- [27] G. W. Fischer, Z. Chem. 1968, 8, 269-270.
- [28] T. Shimada, I. Nakamura, Y. Yamamoto, J. Am. Chem. Soc. 2004, 126, 10546–10547.
- [29] S. Cacchi, G. Fabrizi, P. Pace, J. Org. Chem. 1998, 63, 1001-1011.
- [30] X. Zeng, R. Kinjo, B. Donnadieu, G. Bertrand, Angew. Chem. Int. Ed. 2010, 49, 942–945; Angew. Chem. 2010, 122, 954.
- [31] T. D. Cook, P. E. Fanwick, T. Ren, Organometallics 2014, 33, 4621–4624.
- [32] E. C. Judkins, M. Zeller, T. Ren, *Inorg. Chem.* 2018, 57, 2249–2259; P. U. Thakker, R. G. Aru, C. Sun, W. T. Pennington, A. M. Siegfried, E. C. Marder, P. S. Wagenknecht, *Inorg. Chim. Acta* 2014, 411, 158–164.
- [33] B. M. Oxley, B. Mash, M. Zeller, S. Banziger, T. Ren, Acta Crystallogr., Sect. E 2018, 74, 522–529.
- [34] P. U. Thakker, C. Sun, L. Khulordava, C. D. McMillen, P. S. Wagenknecht, J. Organomet. Chem. 2014, 772, 107–112.
- [35] W. A. Hoffert, M. K. Kabir, E. A. Hill, S. M. Mueller, M. P. Shores, *Inorg. Chim. Acta* 2012, 380, 174–180.
- [36] T. D. Cook, S. N. Natoli, P. E. Fanwick, T. Ren, Organometallics 2015, 34, 686–689.
- [37] T. D. Cook, S. N. Natoli, P. E. Fanwick, T. Ren, Organometallics 2016, 35, 1329–1338; S. N. Natoli, T. D. Cook, T. R. Abraham, J. J. Kiernicki, P. E. Fanwick, T. Ren, Organometallics 2015, 34, 5207–5209; S. N. Natoli, T. J. Azbell, P. E. Fanwick, M. Zeller, T. Ren, Organometallics 2016, 35, 3594–3603.
- [38] Y. Liu, H.-Y. Wang, G. Chen, X.-P. Xu, S.-J. Ji, *Aust. J. Chem.* **2009**, *62*, 934–940
- [39] M. Chrominski, A. Lewalska, D. Gryko, Chem. Commun. 2013, 49, 11406– 11408.
- [40] M. Younus, N. J. Long, P. R. Raithby, J. Lewis, N. A. Page, A. J. P. White, D. J. Williams, M. C. B. Colbert, A. J. Hodge, M. S. Khan, D. G. Parker, J. Organomet. Chem. 1999, 578, 198–209.
- [41] B. Bosnich, M. L. Tobe, G. A. Webb, *Inorg. Chem.* **1965**, *4*, 1109–1112.
- [42] APEX3 v2016.9-0, Saint V8.34A, Saint V8.37A; 2016.
- [43] SHELXTL suite of programs, version 6.14; 2000–2003; G. M. Sheldrick, Acta Crystallogr., Sect. A 2008, 64, 112–122.
- [44] G. M. Sheldrick, Acta Crystallogr., Sect. C 2015, 71, 3–8; C. B. Hübschle, G. M. Sheldrick, B. Dittrich, J. Appl. Crystallogr. 2011, 44, 1281–1284.

Received: October 4, 2019